

Probing relativistic spin effects in the nucleon by means of Drell–Yan processes

F. Cano¹, P. Faccioli^{2,3} and M. Traini^{1,4}

¹*Dipartimento di Fisica, Università degli Studi di Trento
I-38050 Povo, Italy*

²*ECT* (European Centre for Theoretical Nuclear Physics and Related Areas),
Villa Tambosi, I-38050 Villazzano (Trento), Italy*

³*Department of Physics and Astronomy,
State University of New York at Stony Brook, USA.*

⁴*Istituto Nazionale di Fisica Nucleare, G.C. Trento.
(February 1, 2008)*

Significant differences between transverse and longitudinal polarized parton distributions are found at low energies within a light-front covariant quark model of the nucleon. These differences are due to relativistic spin effects introduced by the Melosh rotations and survive evolution to higher Q^2 scales. A specific observable related to double-spin asymmetries in lepton pair production in polarized hadron-hadron collisions is defined. The possibility of assessing the relevance of these relativistic spin effects in future experiments at RHIC and HERA- \vec{N} is discussed.

I. INTRODUCTION

A complete description of the momentum and spin degrees of freedom of quarks and antiquarks in the nucleon requires, at leading twist, the definition of three sets of parton distributions. Two of them, the momentum distribution $f_1(x, Q^2)$ and the helicity distribution $g_1(x, Q^2)$, have been intensively investigated in the last few years (for recent reviews see [1,2]) while the so called transversity distribution, $h_1(x, Q^2)$, has come to the attention of theorists and experimentalists more recently in the analysis of Drell–Yan spin asymmetries [3]. The main reason why it has passed unnoticed for such a longtime is related to its chiral-odd character. If quark masses are neglected in the QCD Lagrangian, no interaction at lowest order of perturbation theory, can flip chirality. As a consequence, transversity is strongly suppressed (by powers of m_q/Q) in deep inelastic lepton-nucleon scattering (DIS) and in general in any hard process that involves only one parton distribution. In hadron-hadron collisions the chirality of the partons that annihilate is uncorrelated and the previous restrictions do not apply.

Recently there has been a number of proposals to measure the transversity parton distributions (see [4] for a review). Lepton pair production in doubly polarized Drell–Yan processes are among the proposed scenarios and such experiments are included in the research program at RHIC and the HERA- \vec{N} project [5]. The feasibility of measurements of double transverse asymmetries (A_{TT}) at polarized pp colliders (RHIC) and fixed-target experiments (HERA- \vec{N}) has been recently studied [6]. The expected maximal value for A_{TT} at the kinematic range covered by RHIC is around 1-2 %, which would be difficult to measure with the present acceptances. For HERA- \vec{N} , A_{TT} is expected to reach values as large as 5 %.

Along with the experimental prospects, many efforts have also been made on the theoretical side [7–12]. In particular Jaffe and Ji calculated h_1 within the Bag Model of the nucleon [7], pointing out the relativistic character of the differences between transverse and longitudinal polarization properties.

The calculation of leading order (LO) [13] and next-to-leading order (NLO) [14] anomalous dimensions allowed to address quantitatively the differences between g_1 and h_1 due to perturbative QCD (pQCD) evolution in different models [10,11]. In particular, Scopetta and Vento have shown that pQCD differences are sizeable only for low values of x ($x \lesssim 0.1$) [10].

On the other hand the boundary conditions of the evolution equations, that are provided by the low energy input at the hadronic scale Q_0^2 ($\lesssim 1 \text{ GeV}^2$), can yield an additional, non perturbative, difference. As it was stressed by Jaffe and Ji [7], at this scale the equality $h_1(x, Q_0^2) = g_1(x, Q_0^2)$ is a typical outcome of non-relativistic models of the nucleon, in which motion and spin observables are uncorrelated. In other words, any departure from the previous identity is a signature of relativity in the employed hadronic model. A complete theoretical study of h_1 and g_1 has to account for both: the relativistic effects which distinguish h_1 from g_1 at the non-perturbative scale, and the pQCD evolution which differs for the two structure functions.

Aim of the present work is the quantitative study of the relativistic effects in h_1 and g_1 due to the correlations of spin and parton motion in the hadronic systems. For this purpose we use light-front dynamics formalism in which

the interplay between motion and spin is made explicit through the Melosh rotations. In particular, we make use of the light-front covariant (LFC) quark model of ref. [15] to compute the leading twist contribution to the matrix elements at the hadronic scale Q_0^2 . The non-perturbative input is then evolved, at NLO, up to a higher Q^2 scale. We shall show that relativistic corrections introduced at Q_0^2 clearly survive evolution. Measurements of observables involving transverse and longitudinal asymmetries might put in evidence the corrections to the naive non-relativistic spin picture adopted in low-energy models of the nucleon.

The paper is organized as follows: in section II the framework to calculate h_1 and g_1 within the LFC quark model is described and a specific observable, related to double spin asymmetry experiments, is defined. The definition is such that the view on relativistic spin effects is optimized. Results in the kinematic range covered by RHIC and HERA- \vec{N} are presented in section III, where the feasibility of the detection of these effects is also discussed. Finally, conclusions are drawn in section IV.

II. POLARIZED PARTON DISTRIBUTIONS IN A LFC QUARK MODEL

A. Polarized partons at the hadronic scale

The helicity distribution $g_1^a(x, Q^2)$ of a parton with flavour a is defined as the probability of having a (longitudinally) polarized parton a with spin parallel to the longitudinal polarization of the parent nucleon minus the probability of finding the parton polarized in the opposite direction. A similar definition applies to $h_1^a(x, Q^2)$ for transverse polarizations [2].

In the quark model a simple approach can be developed to connect parton and momentum densities at the hadronic scale Q_0^2 where valence degrees of freedom dominate the matrix elements at leading twist [16]. In particular, g_1^a [15,16] and h_1^a [10] can be related to the longitudinal and transverse quark momentum densities respectively. Namely:

$$g_1^a(x, Q_0^2) = \frac{1}{(1-x)^2} \int d^3k (n_a^\uparrow(\vec{k}) - n_a^\downarrow(\vec{k})) \delta\left(\frac{x}{1-x} - \frac{k^+}{M/\sqrt{2}}\right), \quad (1)$$

$$h_1^a(x, Q_0^2) = \frac{1}{(1-x)^2} \int d^3k (n_a^{\rightarrow}(\vec{k}) - n_a^{\leftarrow}(\vec{k})) \delta\left(\frac{x}{1-x} - \frac{k^+}{M/\sqrt{2}}\right), \quad (2)$$

where \vec{k} is the three-momentum of the struck quark, M is the nucleon mass, $k^+ = (\sqrt{\vec{k}^2 + m_q^2} + k_z)/\sqrt{2}$ and $n_a^{\uparrow(\downarrow)}(\vec{k})$ is the density of (valence) quarks with momentum \vec{k} and longitudinal polarization aligned (antialigned) with the longitudinal polarization of the parent nucleon. A similar notation ($n_a^{\rightarrow}(\vec{k})$) is used for transverse polarization. The explicit expressions for the densities are:

$$n_a^{\uparrow\downarrow}(\vec{k}) = \langle P, S_z = +1/2 | \sum_{i=1}^3 \mathcal{P}_i^a \frac{1 \pm \sigma_z^{(i)}}{2} \delta(\vec{k} - \vec{k}_i) | P, S_z = +1/2 \rangle, \quad (3)$$

$$n_a^{\rightarrow\leftarrow}(\vec{k}) = \langle P, S_x = +1/2 | \sum_{i=1}^3 \mathcal{P}_i^a \frac{1 \pm \sigma_x^{(i)}}{2} \delta(\vec{k} - \vec{k}_i) | P, S_x = +1/2 \rangle, \quad (4)$$

where \mathcal{P}_i^a is the flavour projector.

In any non-relativistic description of the wave function the densities (3) and (4) are equal and hence $h_1(x, Q_0^2) = g_1(x, Q_0^2)$ as discussed by Jaffe and Ji [7]. However the degeneracy is removed by relativistic covariance requirements, such as those which are implemented in the covariant quark models based on light-front dynamics [15].

Light-front dynamics with a fixed number of particles has been widely discussed in the literature (see [17] for reviews), so that it is enough to highlight briefly the main features of the angular momentum in this formalism. In relativistic quantum theories, the angular momentum operator is obtained from the generators of the Poincaré group. In the light front form of the dynamics problems arise when considering addition of angular momenta, because usual composition rules are not satisfied. Nevertheless, it is possible to restore them by means of a unitary transformation: the Melosh rotation [18]. From the physical viewpoint these transformations relate the angular momentum eigenstates in a subsystem rest frame (a quark, for example) to the centre of mass frame. For spin 1/2 particles the Melosh rotations (MR) that link light-front to canonical spin states are represented by:

$$D^{1/2}[R_M(\vec{k})] = \frac{(m + \omega + k_z) - i\vec{\sigma} \cdot (\hat{z} \times \vec{k}_\perp)}{((m + \omega + k_z)^2 + \vec{k}_\perp^2)^{1/2}}, \quad (5)$$

where \vec{k} is the three-momentum of the particle and $\omega = \sqrt{\vec{k}^2 + m^2}$ its relativistic energy. The fact that $D^{1/2}[R_M(\vec{k})] \rightarrow 1$ in the limit $\vec{k}_\perp \rightarrow 0$ reveals the relativistic origin of the MR. A new spin-flavor basis is then defined (the Pauli-Melosh basis) in which the ordinary (canonical) Pauli spinors for each individual particle are replaced by the Melosh-rotated spinors:

$$\chi_i = D^{1/2}[R_M(\vec{k}_i)]\chi_i^c = \frac{(m_i + \omega_i + k_{i_z}) - i\vec{\sigma}^{(i)} \cdot (\hat{z} \times \vec{k}_{i_\perp})}{((m_i + \omega_i + k_{i_z})^2 + \vec{k}_{i_\perp}^2)^{1/2}}\chi_i^c, \quad (6)$$

where χ_i^c are the usual (canonical) Pauli spinors for the particle i . The Pauli-Melosh basis constitutes a 'minimal' relativistic spin basis [19] that, despite of its non-manifest covariance, is compatible with Poincaré invariance requirements.

In our calculation we shall refer to the wave function Ψ of ref. [15], where the relativistic mass equation:

$$(M_0 + V) \Psi \equiv \left(\sum_{i=1}^3 \sqrt{\vec{k}_i^2 + m_i^2} + V \right) \Psi = E \Psi \quad (7)$$

has been solved. The free relativistic mass operator $M_0 = \sum_{i=1}^3 \omega_i$ is supplemented with an hypercentral phenomenological interaction

$$V = -\frac{\tau}{\xi} + \kappa_l \xi + \Delta, \quad (8)$$

where the hyper-radius $\xi^2 = \sum_{i=1}^3 (\vec{r}_i - \vec{R})^2$ is a function of what, in a non relativistic treatment, is the vector position of the particles \vec{r}_i and the center of mass position \vec{R} . τ , κ_l and Δ are constants fixed to reproduce the basic features of the low-energy baryonic spectrum pattern in the $J^P = 1/2^\pm$ channels. Since this interaction is invariant under rotations and does not depend on the total light-front momentum, all the commutation relations that guarantee the covariance requirement (see [17]) are correctly satisfied. The advantage of the hypercentral interactions, well known in the non-relativistic limit [20], is that they allow a straightforward solution of the Schrödinger equation. The resulting spin-isospin wave function is $SU(6)$ symmetric. It should be emphasized that the degeneracy between h_1 and g_1 in the non-relativistic limit is independent of the presence of $SU(6)$ -breaking terms in the nucleon wave function.

From eq. (6) it is evident the correlation between spin and motion in the Pauli-Melosh spin basis, so that the momentum densities (3) and (4) are no longer equal, independently of its $SU(6)$ -symmetric character. Differences between $h_1^a(x, Q_0^2)$ and $g_1^a(x, Q_0^2)$ are now proportional to the internal transverse momentum \vec{k}_\perp , as expected:

$$\begin{aligned} h_1^u(x, Q_0^2) - g_1^u(x, Q_0^2) &= -4(h_1^d(x, Q_0^2) - g_1^d(x, Q_0^2)) \\ &= \frac{1}{(1-x)^2} \int d^3k \left[\frac{4}{9} \frac{\vec{k}_\perp^2}{(m + \omega + k_z)^2 + \vec{k}_\perp^2} \right] \\ &\quad \times n(\vec{k}) \delta \left(\frac{x}{1-x} - \frac{k^+}{M/\sqrt{2}} \right), \end{aligned} \quad (9)$$

where $n(\vec{k})$ is the unpolarized flavorless quark momentum density normalized to the number of particles as obtained by solving the mass equation (7). Equation (9) is one of the central results of the present work. It shows that differences between h_1^a and g_1^a have a clear relativistic origin depending on the kinematical structure of the MR. The x -dependence of the quantity $h_1^a - g_1^a$ is embodied in the wave function term $n(\vec{k})$. Within a fully non-relativistic approach $h_1^a - g_1^a$ would vanish and the actual (and identical) values of h_1^a and g_1^a would be largely suppressed for $x \gtrsim 0.5$ due to the lack of high momentum components in $n(\vec{k})$ for typical non-relativistic models [21]. In fact the relativistic effects show up, in the present approach, in a twofold way: i) MR introduce the non-vanishing difference $h_1^a - g_1^a$ of eq.(9); ii) high momentum components in $n(\vec{k})$ which are mostly originated by the relativistic kinetic energy in the mass equation (7) and that reinforce the MR contribution, as discussed in ref. [15] for g_1^a .

Concerning the scale dependence, it should be stressed that eq.(9) is valid at a low-energy (hadronic) scale Q_0^2 , where the non-perturbative models used to calculate the twist-two matrix elements can be applied. At higher (experimental) scales $Q^2 > Q_0^2$ perturbative QCD evolution yields an additional contribution to the differences between longitudinal and transverse polarization observables (cfr. section III). Previous attempts [8] to study the effects of MR in h_1 disregarded this scale dependence and did not include perturbative contributions.

B. Double Spin Asymmetries

Let us now discuss a specific combination of longitudinally and transversely polarized parton distributions, namely the ratio

$$R_{TL}(x_1, x_2, Q^2) = \frac{\sum_a e_a^2 h_1^a(x_1, Q^2) h_1^{\bar{a}}(x_2, Q^2) + (x_1 \leftrightarrow x_2)}{\sum_a e_a^2 g_1^a(x_1, Q^2) g_1^{\bar{a}}(x_2, Q^2) + (x_1 \leftrightarrow x_2)}, \quad (10)$$

where e_a is the charge of a quark of flavour a . The arguments x_1 and x_2 are related, for Drell-Yan processes, to the center of mass energy \sqrt{s} , the invariant mass of the produced lepton pair Q^2 , and the rapidity $y = \arctan(Q^3/Q^0)$:

$$x_1 = \sqrt{\frac{Q^2}{s}} e^y \quad x_2 = \sqrt{\frac{Q^2}{s}} e^{-y}. \quad (11)$$

$R_{TL}(x_1, x_2, Q^2)$ does not depend on the unpolarized parton distribution and involves only the ratio between g_1 and h_1 . To this respect it is less model dependent than the single terms and is quite transparent for studying MR effects.

The flavor combination of transverse parton distributions in Eq. (10) appears in the LO double transverse asymmetry of Drell-Yan processes:

$$\begin{aligned} A_{TT}|_{LO} &= \frac{\frac{d\sigma(\overrightarrow{})}{dQ^2 dy d\phi} - \frac{d\sigma(\overleftarrow{})}{dQ^2 dy d\phi}}{\frac{d\sigma(\overrightarrow{})}{dQ^2 dy} + \frac{d\sigma(\overleftarrow{})}{dQ^2 dy}} \Big|_{LO} = \\ &= \frac{\cos 2\phi}{4\pi} \left(\frac{\sum_a e_a^2 h_1^a(x_1, Q^2) h_1^{\bar{a}}(x_2, Q^2) + (x_1 \leftrightarrow x_2)}{\sum_a e_a^2 f_1^a(x_1, Q^2) f_1^{\bar{a}}(x_2, Q^2) + (x_1 \leftrightarrow x_2)} \right), \end{aligned} \quad (12)$$

where the arrows denote the transverse polarization of the beam and target and θ (ϕ) is the polar (azimuthal) angle of the detected lepton.

The corresponding LO asymmetry with longitudinally polarized hadrons, A_{LL} , is proportional to the combination of helicity distributions g_1 considered in Eq. (10):

$$A_{LL}|_{LO} = \frac{\frac{d\sigma(\uparrow\downarrow)}{dQ^2 dy} - \frac{d\sigma(\uparrow\uparrow)}{dQ^2 dy}}{\frac{d\sigma(\uparrow\downarrow)}{dQ^2 dy} + \frac{d\sigma(\uparrow\uparrow)}{dQ^2 dy}} \Big|_{LO} = \frac{\sum_a e_a^2 g_1^a(x_1, Q^2) g_1^{\bar{a}}(x_2, Q^2) + (x_1 \leftrightarrow x_2)}{\sum_a e_a^2 f_1^a(x_1, Q^2) f_1^{\bar{a}}(x_2, Q^2) + (x_1 \leftrightarrow x_2)}, \quad (13)$$

Then, R_{TL} is just the ratio between double transverse and double longitudinal asymmetries at LO:

$$R_{TL} = \frac{4\pi}{\cos 2\phi} \frac{A_{TT}|_{LO}}{A_{LL}|_{LO}} \quad (14)$$

The evolution procedure we are going to use is a NLO procedure and therefore the parton distribution and the corresponding cross sections should be consistently evaluated at NLO. As a consequence the asymmetries do not assume the simple forms (12) and (13). Nevertheless it is still feasible to establish a rather close connection between the combinations that enter Eq. (10) and the NLO asymmetries.

Indeed, the differential cross section for longitudinally polarized process is written, at NLO, as [22]:

$$\begin{aligned} \frac{d\sigma(\uparrow\downarrow)}{dQ^2 dy} - \frac{d\sigma(\uparrow\uparrow)}{dQ^2 dy} \Big|_{NLO} &= \frac{4\pi\alpha_{em}^2}{9sQ^2} \int dx_1 dx_2 \{ \\ &\left(\sum_a e_a^2 g_1^a(x_1, Q^2) g_1^{\bar{a}}(x_2, Q^2) \right) \left(\Delta c_{q\bar{q}}^{\text{DY}(0)} + \frac{\alpha_s(Q^2)}{2\pi} \Delta c_{q\bar{q}}^{\text{DY}(1)} \right) \\ &+ \Delta G(x_1, Q^2) \sum_a e_a^2 (g_1^a(x_2, Q^2) + g_1^{\bar{a}}(x_2, Q^2)) \frac{\alpha_s(Q^2)}{2\pi} \Delta c_{qg}^{\text{DY}(1)} \\ &+ (x_1 \leftrightarrow x_2) \} , \end{aligned} \quad (15)$$

where $\Delta G(x, Q^2)$ is the polarization of gluons and the coefficient $\Delta c_{q\bar{q}}^{\text{DY}(0)} = \delta(x_1 - \sqrt{\frac{Q^2}{s}} e^y) \delta(x_2 - \sqrt{\frac{Q^2}{s}} e^{-y})$. The NLO order coefficients are explicitly given in [22]. The NLO order introduces on the one hand the polarization

of the gluons due to the subprocess $qg \rightarrow q\gamma$ and on the other hand the coefficients $\Delta c_{q\bar{q},qg}^{\text{DY}(1)}$ that contain terms which are not proportional to $\delta(x_1 - \sqrt{\frac{Q^2}{s}}e^y)\delta(x_2 - \sqrt{\frac{Q^2}{s}}e^{-y})$ and therefore break the relationship (11) we have used in our calculation. A similar modification appears for the unpolarized DY cross section. Nevertheless, an estimation of the asymmetry A_{LL} by using available parameterization of polarized parton distributions indicate that the NLO asymmetry is dominated by the $O(\alpha_s^0)$ of the $q\bar{q} \rightarrow \gamma$ subprocess in the central rapidity region. This term contains just the combination of polarized parton distributions that we are interested in and which enters in the ratio (10). Alternatively, it would also be possible to extract this combination of helicity parton distributions from other experiments.

In the transversely NLO polarized cross sections, gluons are absent since there is no equivalent 'transversity' for gluons, and hence [23]:

$$\left. \frac{d\sigma(\overrightarrow{})}{dQ^2 dy d\phi} - \frac{d\sigma(\overleftarrow{})}{dQ^2 dy d\phi} \right|_{\text{NLO}} = \frac{\alpha_{\text{em}}^2}{9sQ^2} \cos(2\phi) \int dx_1 dx_2 \{$$

$$\left(\sum_a e_a^2 h_1^a(x_1, Q^2) h_1^{\bar{a}}(x_2, Q^2) \right) \left(\delta c_{q\bar{q}}^{\text{DY}(0)} + \frac{\alpha_s(Q^2)}{2\pi} \delta c_{q\bar{q}}^{\text{DY}(1)} \right)$$

$$+ (x_1 \leftrightarrow x_2) \} \quad . \quad (16)$$

Though the cross section is proportional to the combination of transversity distributions that we have used in (10), the NLO order coefficient $\delta c_{q\bar{q}}^{\text{DY}(1)}$ may spoil the relationship (11) again. However, it was shown in ref. [23], that the dominant term in this coefficient (and in the equivalent one for the unpolarized cross section) is proportional to $\delta(x_1 - \sqrt{\frac{Q^2}{s}}e^y)\delta(x_2 - \sqrt{\frac{Q^2}{s}}e^{-y})$, so that it is still possible a rather direct extraction of the combination $\sum_a e_a^2 h_1^a(x_1, Q^2) h_1^{\bar{a}}(x_2, Q^2)$ from the analysis of the transverse asymmetry at NLO.

III. RESULTS

A. Parton distributions: non-perturbative and perturbative contributions

To reach the experimental regime we have evolved the calculated parton distributions from the hadronic scale up to a scale $Q^2 > Q_0^2$ by using pQCD at NLO, in the $\overline{\text{MS}}$ scheme. The sensitivity to the factorization scheme in this approach has been tested in previous calculations [15] and found to be generally small.

The value of Q_0^2 (the hadronic scale) is fixed [16] by evolving backwards the parametrized experimental fits for unpolarized parton distributions [24], to the scale where the valence quarks carry the whole momentum of the nucleon. We found $Q_0^2 = 0.094 \text{ GeV}^2$ and the reliability of the pQCD evolution procedure at such low scale was studied in detail in [10,15,16].

Let us emphasize that the value $Q_0^2 = 0.094 \text{ GeV}^2$ is found by using an evolution code where the transcendental equation

$$\ln \frac{Q^2}{\Lambda_{\text{NLO}}^2} - \frac{4\pi}{\beta_0 \alpha_s(Q^2)} + \frac{\beta_1}{\beta_0^2} \ln \left[\frac{4\pi}{\beta_0 \alpha_s(Q^2)} + \frac{\beta_1}{\beta_0^2} \right] = 0 \quad (17)$$

has been solved to get the NLO coupling constant. The use of the full NLO expression (17) is mandatory when evolving from/to a low energy scale [25] and the approximate solution

$$\alpha_s(Q^2) = \frac{1}{\beta_0 \ln(Q^2/\Lambda_{\text{NLO}}^2)} \left[1 - \frac{\beta_1}{\beta_0^2} \frac{\ln \ln(Q^2/\Lambda_{\text{NLO}}^2)}{\ln(Q^2/\Lambda_{\text{NLO}}^2)} \right] , \quad (18)$$

which is valid for large values of $Q^2/\Lambda_{\text{NLO}}^2$ and often used in NLO codes (e.g. ref. [26]), would introduce quite spurious effects. In particular, the evolution to energy scales as low as the hadronic point Q_0^2 may yield a negative gluon contribution at Q_0^2 , related to a large extent to the spurious effects introduced by eq.(18). In the present case, for example, evolving back the experimental fit [24] to the hadronic scale $Q_0^2 = 0.094 \text{ GeV}^2$, would give a fraction of momentum carried by the gluons of -1.44×10^{-2} , which, although non-zero, is relatively small. Obviously, the situation is much worse when Eq. (18) is used instead of Eq. (17).

In addition, the evolution code to be used for hadronic model calculations must guarantee complete symmetry for the forward and backward paths $Q_0^2 \rightarrow Q^2$ and vice versa, as implied by genuine perturbative QCD expansion at

NLO. Additional approximations associated with Taylor expansion valid for large Q^2/Λ_{NLO}^2 , must be avoided, as discussed in [16].

In Fig. 1 we show the curves for h_1^u and g_1^u at the hadronic scale Q_0^2 (Fig. 1(a)) and at the partonic scale $Q^2 = 100 \text{ GeV}^2$ (Fig. 1(b)). A remarkable difference between $xh_1(x, Q_0^2)$ and $xg_1(x, Q_0^2)$ appears at large x , reaching a peak at $x \approx 0.5$. Quantitatively they are bigger than those obtained within bag models [7,10]. It is clear that the probability of transverse polarization is larger than the longitudinal one when relativistic effects are considered.

It is possible to appreciate better the MR effects by simply setting $D^{1/2}[R_M(\vec{k})] \rightarrow 1$. In this case the remaining relativistic ingredient is the high momentum components generated by the 'relativized' Schrödinger equation (7). The results are also shown in Fig. 1(a) and we get $h_1(x, Q_0^2) = g_1(x, Q_0^2)$ as expected. After evolution (Fig. 1(b)) we see that when the MR are neglected, g_1 and h_1 differ mainly at low x ($x \lesssim 0.1$) because of pQCD evolution [10,11], while the inclusion of the correlations between spin and motion produce large effects also in the medium and large x region.

In order to study the effects of MR in the combination of polarized parton distributions we are interested in, let us first consider the ratios

$$R_L = \frac{\sum_a e_a^2 g_1^a(x_1, Q^2) g_1^{\bar{a}}(x_2, Q^2) + (x_1 \leftrightarrow x_2)}{\sum_a e_a^2 f_1^a(x_1, Q^2) f_1^{\bar{a}}(x_2, Q^2) + (x_1 \leftrightarrow x_2)} \quad (19)$$

and

$$R_T = \frac{\sum_a e_a^2 h_1^a(x_1, Q^2) h_1^{\bar{a}}(x_2, Q^2) + (x_1 \leftrightarrow x_2)}{\sum_a e_a^2 f_1^a(x_1, Q^2) f_1^{\bar{a}}(x_2, Q^2) + (x_1 \leftrightarrow x_2)} \quad (20)$$

shown in Fig. 2(a) and Fig. 2(b) respectively as a function of the center of mass rapidity y in a kinematic region ($\sqrt{s} = 100 \text{ GeV}$, $Q^2 = 100 \text{ GeV}^2$) accessible by RHIC experiments. These values are of the order of a few percent, compatible with those obtained in the literature (see for instance [11], where antiquarks are considered also at the hadronic scale). Again it is possible to single out the contribution introduced by MR switching them off. In general, MR reduce both R_T and R_L but this reduction is far more significant for R_L .

In Fig. 3 we show the ratio $R_{TL} = R_T/R_L$ as a function of y (in the same kinematical region) when considering Melosh rotations and when they are neglected. Figure 3 represents our reference point to assess the importance of relativistic spin effects: they enhance the transverse ratio R_T with respect to the longitudinal term R_L . Namely, if Melosh rotations are taken into account $R_T \simeq R_L$ in the considered kinematic regime. On the contrary, if the spin-motion correlations are neglected (non-relativistic limit), then in the same region $R_T \simeq \frac{1}{2}R_L$. Experiments may decide between these two alternatives, therefore probing the relevance of covariance effects in the dynamical description of the nucleon spin.

Before examining the possibility of measuring these effects let us discuss some issues concerning the previous results: the coupling of g_1 to the polarized gluons in the evolution at NLO and the dependence of R_{TL} on the spatial nucleon wave function.

B. LO versus NLO evolution

In our valence model of the nucleon, the contribution to $g_1^{\bar{q}}(x, Q^2)$ and $h_1^{\bar{q}}(x, Q^2)$ comes from evolution only. On qualitative grounds one would expect $h_1^{\bar{q}}(x, Q^2) \ll g_1^{\bar{q}}(x, Q^2)$ (i.e. $R_{TL} \ll 1$), since $h_1^{\bar{q}}$ at LO vanishes while $g_1^{\bar{q}}$ receives contributions also from the lowest order in α_s . However, a careful analysis shows that this is not necessarily the case, since the final value of $g_1^{\bar{q}}(x, Q^2)$ is not only determined by the order of α_s but also from the behavior of the anomalous dimensions. More specifically, in order to understand why one gets $g_1^{\bar{q}}(x, Q^2) \approx h_1^{\bar{q}}(x, Q^2)$, let us consider the DGLAP equations for the longitudinally polarized parton distributions [27] to disentangle the coupling of $g_1^{\bar{q}}$ to quarks, antiquarks and gluons¹:

$$\frac{\partial}{\partial \ln Q^2} \Delta q_{NS}(x, Q^2) = \frac{\alpha_s(Q^2)}{2\pi} \Delta P_{q^{\pm}, NS}(x) \otimes \Delta q_{NS}(x, Q^2) \quad (21)$$

$$\frac{\partial}{\partial \ln Q^2} \begin{pmatrix} \Delta q_s(x, Q^2) \\ \Delta g(x, Q^2) \end{pmatrix} = \frac{\alpha_s(Q^2)}{2\pi} \begin{pmatrix} \Delta P_{qq}(x, Q^2) & \Delta P_{qg}(x, Q^2) \\ \Delta P_{gq}(x, Q^2) & \Delta P_{gg}(x, Q^2) \end{pmatrix} \otimes \begin{pmatrix} \Delta q_s(x, Q^2) \\ \Delta g(x, Q^2) \end{pmatrix} \quad (22)$$

¹This kind of analysis is far more cumbersome in the evolution procedure based on the RGE.

where $\Delta q_s = \sum_a (g_1^a + g_1^{\bar{a}})$ and Δq_{NS} corresponds to non-singlet combinations of g_1^a and $g_1^{\bar{a}}$. For the sake of simplicity we will give results for $\frac{\partial g_1^{\bar{u}}(x, Q^2)}{\partial \ln Q^2}$ at $Q^2 = 100 \text{ GeV}^2$ (conclusions are not changed for other Q^2 points we have checked) at LO.

In Fig. 4 we show the contribution to the derivative of $g_1^{\bar{u}}$ due to the coupling to $\Delta G(x, Q^2)$ and to the terms proportional to the quarks and antiquarks at LO. The remarkable feature is the opposite sign of the coupling to the gluons and to the quarks+antiquarks at LO that makes the final derivative be not too large for $x \gtrsim 0.05$. This partial cancellation between different contributions produces a rather slow increase of $g_1^{\bar{u}}(x, Q^2)$ with Q^2 at order $(\alpha_s/2\pi)$ and the final value of $g_1^{\bar{u}}(x, Q^2)$ at NLO are comparable to that of $h_1^{\bar{u}}(x, Q^2)$. This happens for $x \gtrsim 0.05$, while for smaller x the growing of $g_1^{\bar{u}}$ dominates over that of $h_1^{\bar{u}}$, due to some extent to the large size of the coupling to gluons, which is absent in the evolution of $h_1^{\bar{u}}$.

It should be reminded that R_{TL} vanishes at leading order since the sea quarks are entirely generated through evolution. This fact prevent us from doing a quantitative comparison between the LO and NLO for R_{TL} . However, Scopetta and Vento [10] analyzed the LO and NLO evolution for other flavour combinations of h_1 and g_1 and it was found that these differences between LO and NLO were not too large and went in the same direction for g_1 and h_1 .

C. Quark model dependence

At this point one can argue that these results for $R_{TL}(x_1, x_2, Q^2)$ could be strongly influenced by the presence of high momentum components in the spatial part of the wave function, carried over by the presence of a relativistic kinetic energy in the mass operator. These components have been proved to be essential to describe electromagnetic transitions and elastic form factors [28] and also the high x region in DIS [15,16]. We have therefore repeated the calculation of the ratio $R_{TL}(x_1, x_2, Q^2)$ starting from a nucleon wave function obtained by making use of a non-relativistic kinetic energy in the mass operator (cfr. eq. (7)). The interaction has been kept of the same form (8), while the values of the parameters (τ , κ_l , Δ) have been reset according to ref [15].

The corresponding result for $R_{TL}(x_1, x_2, Q^2)$ is shown also in Fig. 3. We can see that the ratio obtained from a fully non-relativistic model, lies reasonably close to the curve obtained employing a relativistic kinetic energy but neglecting Melosh rotations. Hence, we can safely conclude that $R_{TL}(x_1, x_2, Q^2)$ is rather insensitive to the details of the mass operator, but very sensitive to the relativistic spin corrections derived from a light-front dynamics. This is not so evident for the values of R_T or R_L which are roughly doubled by the same change in the mass operator (see Fig. 2). This fact gives support to the suitability of the chosen observable. Moreover, due to this insensitivity to the details of the spatial wave function, we do not expect a dramatic change of our conclusions for other more sophisticated potential models [29].

D. Experimental detection of relativistic spin effects

In order to study the feasibility of the experimental detection of the differences for R_{TL} we have to estimate the expected errors for R_{TL} under the conditions of RHIC and HERA- \vec{N} . We have calculated the statistical errors according to the expression [6]:

$$\delta A_{TT} = \frac{1}{P_B P_T \sqrt{\mathcal{L} \int \epsilon d\sigma}} \quad (23)$$

where P_B (P_T) is the degree of polarization of the beam (target), \mathcal{L} is the expected luminosity and ϵ is the efficiency in the detection of events. The unpolarized cross section $d\sigma$ is integrated over bins of Q and y .

For RHIC we have taken [6] $P_B = P_T = 0.7$ and a luminosity of 240 pb^{-1} . The calculated errors for the figure 3 in the central rapidity region largely exceeds the separation between the two main curves, even by assuming a 100 % efficiency and integrating over an interval $\Delta y = 3$ and $\Delta Q = 2$ around the central values. Therefore, these effects will be unlikely to be observed at RHIC.

For HERA- \vec{N} the expected degrees of polarization are [5] $P_B = 0.6$ and $P_T = 0.8$ with a projected luminosity of $\mathcal{L} = 240 \text{ pb}^{-1}$. The center of mass energy will be $\sqrt{s} = 39.2 \text{ GeV}$, corresponding to a $E_{Beam} = 820 \text{ GeV}$. We have checked that, though the error bars are far smaller than those obtained for RHIC, relativistic spin effects cannot be disentangled for R_{TL} in the region $Q = 3 \text{ GeV}$, $y = 0$.

In order to maximize the rates we will integrate over the whole range of y :

$$R_{TL}(Q^2) = \frac{\int (\sum_a e_a^2 h_1^a(x_1, Q^2) h_1^{\bar{a}}(x_2, Q^2) + (x_1 \leftrightarrow x_2)) dy}{\int (\sum_a e_a^2 g_1^a(x_1, Q^2) g_1^{\bar{a}}(x_2, Q^2) + (x_1 \leftrightarrow x_2)) dy} . \quad (24)$$

The results for this ratio for the kinematics of HERA- \vec{N} are shown in figure 5, where we can observe the same pattern of differences as the one seen in the y-dependent ratio (Fig. 3). The relative insensitivity to the details of the chosen potential is also evident in this representation. In the error bars shown in Fig. 5 we have taken into account the limited acceptance of the detectors, as explained in [6], which roughly gives $\epsilon = 0.5 - 0.6$ in the considered region. We have also assumed that $\delta\epsilon = \epsilon$. A measurement in the region $Q > 5$ GeV can not single out which is the right spin-flavor basis, while experiments in the low mass region ($Q \approx 3$ GeV) could be more selective, though some overlap between the error bars still persists. For RHIC the acceptance corrections ($\epsilon \approx 0.1 - 0.2$) are too large to reveal relativistic differences.

IV. CONCLUSIONS AND FINAL REMARKS

We have shown that Drell-Yan processes can probe the relativistic effects embodied in a light-front dynamical description of the low energy spin structure of the nucleon. For this purpose, the ratio R_{TL} turns out to be particularly suitable since it is largely independent of the structure of the mass operator and, therefore, of the choice of the phenomenological interaction.

This insensitivity to the details of the spatial degrees of freedom is not so evident for each asymmetry R_T and R_L separately. While predictions for R_{TL} are robust, the given values for R_T and R_L should be considered just at a semiquantitative level. In fact, we have seen that relativistic spin effects would reduce R_T and therefore the chance of measure it with respect to the 'maximal' scenario presented in [6], but no definite quantitative conclusions about the feasibility of measuring transversity should be drawn from Fig. 2.

By estimating the expected statistical errors for RHIC and HERA we have concluded that for HERA- \vec{N} it would be possible to determine the right spin-flavour basis for the nucleon wave function in the low mass region while this kind of measurement would be far more difficult at RHIC.

In the present work we have limited ourselves to give predictions for D-Y related observables in some kinematic regions accessible to RHIC, but the model can be straightforwardly applied to other experimental conditions and to other kind of processes as well. In particular, the observed enhancement of the transverse polarization with respect to the longitudinal one may have some impact in the extraction of the twist-3 contribution to the spin structure function g_2 from DIS experiments [30] (see also [31]).

Finally let us emphasize that we have used a valence quark model to evaluate the parton distributions at the hadronic scale, neglecting sea quark (and antiquark) distributions at that scale. One could argue that the consideration of a non-vanishing $h_1^{\bar{a}}(x, Q_0^2)$ and $g_1^{\bar{a}}(x, Q_0^2)$ would mask the effects due to Melosh rotations. Though a quantitative study of the change in the initial conditions would require more elaborate models (beyond the valence picture [32]) there are, however, some qualitative reasons to support the stability of the results presented in Figs. 3 and 5. A non-vanishing $h_1^{\bar{a}}(x, Q_0^2)$ (and $g_1^{\bar{a}}(x, Q_0^2)$) has two main consequences on the overall scheme: firstly it slightly raises the initial scale Q_0^2 and on the other hand it changes the small x behavior of the parton distributions. The (small) increment of the initial scale would produce a little shift in the Q^2 scale in Fig. 5, but not large enough to give rise to a confusion between the two main curves. With respect to the change of the small x behavior, it should be noticed that in the central rapidity regions we are exploring ranges of x around 0.1 and also for the y-integrated observables this central region is dominant. Furthermore, since we deal with ratios we expect the influence of these changes to be minimized.

ACKNOWLEDGMENTS

We are grateful to S. Scopetta for useful suggestions and for providing us with an updated version of the pQCD evolution code. We thank V. Vento for his encouragement and help during the present study and for a critical reading of the manuscript. We also thank O. Martin for useful correspondence about the calculation of the statistical errors and M. Miyama for sending us his evolution code for h_1 [26].

- [1] M. Anselmino, A. Efremov and E. Leader, Phys. Rep. **261**, 1 (1995); *ibid.* **281**, 399(E) (1997); B. Lampe and E. Reya, hep-ph/9810270, and references therein.
- [2] R.L. Jaffe, in *Proceedings of the Ettore Majorana International School of nucleon Structure, Erice, 1995*, hep-ph/9602236.
- [3] J. Ralston and D.E. Soper, Nucl. Phys. **B152**, 109 (1979).
- [4] R.L. Jaffe, *2nd Topical Workshop Deep Inelastic Scattering off Polarized Targets: Physics with Polarized Targets at HERA, DESY/Zeuthen, 1997*, hep-ph/9710465.
- [5] N. Saito, Nucl. Phys. A **638**, 575 (1998); M. Anselmino *et al.*, *Proceedings of the Workshop on Future Physics at HERA, Hamburg 1995*, hep-ph/9608393.
- [6] O. Martin, A. Schäfer, M. Stratmann and W. Vogelsang, Phys. Rev. D **57**, 3084 (1998); **60**, 117502 (1999).
- [7] R.L. Jaffe and X. Ji, Phys. Rev. Lett. **67**, 552 (1991); Nucl. Phys. **B375**, 527 (1992).
- [8] B.-Q. Ma, I. Schmidt and J. Soffer, Phys. Lett. **B441**, 461 (1998).
- [9] I. Schmidt and J. Soffer, Phys. Lett. **B407**, 331 (1997).
- [10] S. Scopetta and V. Vento, Phys. Lett. **B424**, 25 (1998); hep-ph/9707250.
- [11] V. Barone, T. Calarco and A. Drago, Phys. Lett. **B390**, 287 (1997); Phys. Rev. D **56**, 527 (1997).
- [12] C. Bourrely and J. Soffer, Nucl. Phys. **B423**, 329 (1994); Nucl. Phys. **B445**, 341 (1995); P. Pobylitsa and V. Polyakov, Phys. Lett. **B389**, 350 (1996); B.I. Ioffe and A. Khodjamirian, Phys. Rev. D **51**, 3373 (1995); R. Kirschner, L. Mankiewicz, A. Schäfer and L. Szymanowski, Z. Phys. **C74**, 501 (1997); R. Jakob, P.J. Mulders and J. Rodrigues, Nucl. Phys. **A626**, 937 (1997).
- [13] X. Artru and M. Mekhfi, Z. Phys. **C45**, 669 (1990).
- [14] W. Vogelsang, Phys. Rev. D **57**, 1886 (1998); A. Hayashigaki, Y. Kanazawa and Y. Koike, Phys. Rev. D **56**, 7350 (1997); S. Kumano and M. Miyama, Phys. Rev. D **56**, R2504 (1997).
- [15] P. Faccioli, M. Traini and V. Vento, Nucl. Phys. **A656**, 400 (1999); P. Faccioli, Thesis, Università degli Studi di Trento, 1998.
- [16] M. Traini, V. Vento, A. Mair and A. Zambarda, Nucl. Phys. **A614**, 472 (1997) and references therein; A. Mair and M. Traini, Nucl. Phys. **A624**, 564 (1997).
- [17] B.D. Keister and W.N. Polyzou, Adv. in Nucl. Phys. **20**, 225 (1991); F. Coester, Prog. Part. Nucl. Phys. **29**, 1 (1992); J. Carbonell, B. Desplanques, V.A. Karmanov and J.-F. Mathiot, Phys. Rep. **300**, 215 (1998).
- [18] H. Melosh, Phys. Rev. D **9**, 1095 (1974); M.V. Terent'ev, Sov. J. Nucl. Phys. **24**, 207 (1976); V.B. Berestetskii and M.V. Terent'ev, Sov. J. Nucl. Phys. **24**, 1044 (1976); **25**, 653 (1977).
- [19] M. Beyer, C. Kuhrt and H.J. Weber, Annals Phys. **269**, 129 (1998).
- [20] M. Ferraris, M.M. Giannini, M. Pizzo, E. Santopinto and L. Tiator, Phys. Lett. **B364**, 231 (1995).
- [21] M. Ropele, M. Traini and V. Vento Nucl. Phys. **A584**, 634 (1995); M. Traini, P. Faccioli and V. Vento, Few Body Syst. Suppl. **11**, 347 (1999).
- [22] T. Gehrmann, Nucl. Phys. **B498**, 245 (1997).
- [23] W. Vogelsang and A. Weber, Phys. Rev. D **48**, 2073 (1993).
- [24] H.L. Lai.(CTEQ Coll.), Phys. Rev., D **55**, 1280 (1997).
- [25] T. Weigl and W. Melnitchouk, Nucl. Phys. **B465**, 267 (1996).
- [26] M. Hirai, S. Kumano and M. Miyama, Comput. Phys. Commun. **111**, 150 (1998).
- [27] M. Gluck, E. Reya, M. Stratmann and W. Vogelsang, Phys. Rev. D **53**, 4775 (1996).
- [28] F. Cardarelli, E. Pace, G. Salmè and S. Simula, Phys. Lett. **B357**, 267 (1995); **B371**, 7 (1996).
- [29] S. Caspstick and N. Isgur, Phys. Rev. D **34**, 2809 (1986); L.Ya. Glozman and D.O. Riska, Phys. Rep. **268**, 263 (1996).
- [30] K. Abe et al. (E143 Collaboration), Phys. Rev. Lett. **76**, 587 (1996); P.L. Anthony et al. (E155 Collaboration), Phys. Lett. **B458**, 529 (1999).
- [31] J.L. Cortes, B. Pire and J.P. Ralston, Z. Phys. **C55**, 409 (1992); O. Rondon-Aramayo, private communication.
- [32] F. Cano, P. Faccioli and M. Traini, in preparation.

Figure captions

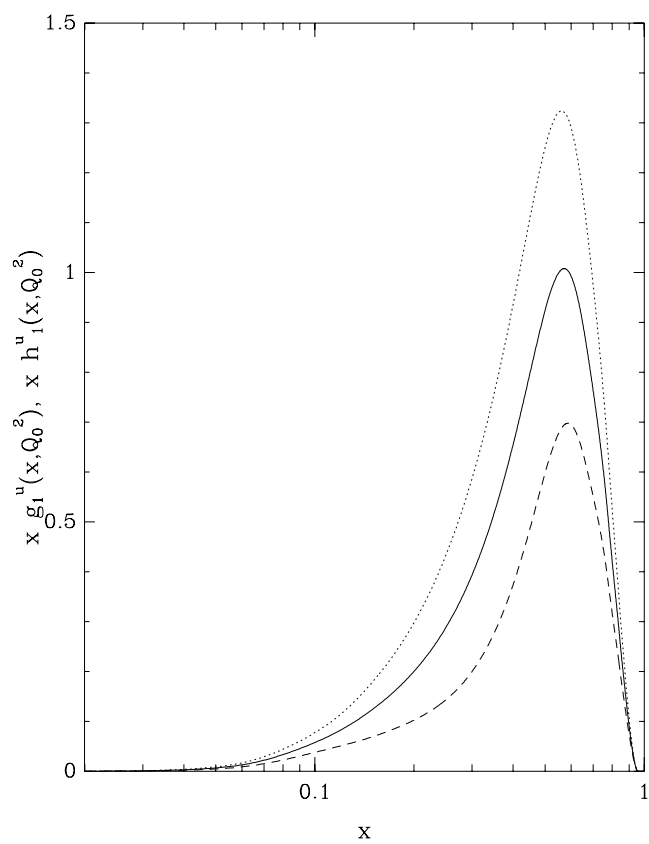
Figure 1 Helicity and transversity distributions for the u quark (a) at the hadronic scale $Q_0^2 = 0.094 \text{ GeV}^2$ and (b) after evolution up to $Q^2 = 100 \text{ GeV}^2$. In fig. a) the solid line corresponds to xh_1 , the dashed line to xg_1 and the dotted line is the result when Melosh rotation is not considered ($h_1 = g_1$). In Fig. (b) the solid and dashed lines represent h_1 and g_1 respectively. The dotted and dash-dotted lines correspond to h_1 and g_1 when Melosh Rotation is neglected.

Figure 2. R_L (a) and R_T (b) ratios as defined in Eqs. (19,20) as a function of the center of mass rapidity y for $Q^2 = 100 \text{ GeV}^2$ and a center of mass energy $\sqrt{s} = 100 \text{ GeV}$ (solid line). The dashed line corresponds to the case when the Melosh rotation is switched off. The dotted line is the result obtained in the non-relativistic model discussed in the text.

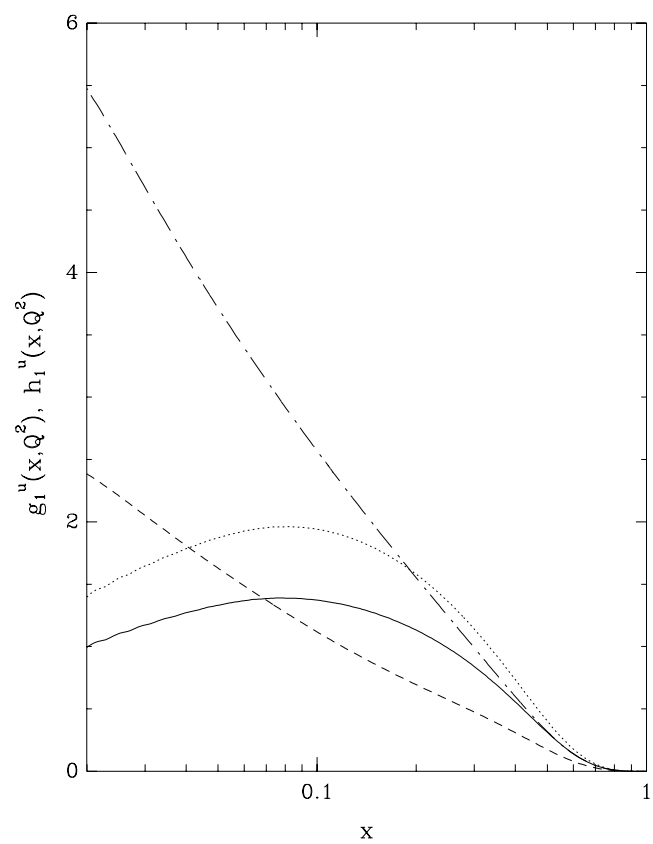
Figure 3. Ratio between transverse and longitudinal parton distributions (eq. (10)) as a function of the center of mass rapidity y for $Q^2 = 100 \text{ GeV}^2$ and a center of mass energy $\sqrt{s} = 100 \text{ GeV}$. Notation as in Fig. 2.

Figure 4. Contributions to $\frac{\partial g_1^{\bar{u}}}{\partial \ln Q^2}$ at LO coming from the terms proportional to the gluons (solid line) and to the quarks + antiquarks (dashed line). All the results correspond to $Q^2 = 100 \text{ GeV}^2$.

Figure 5. Ratio between transverse and longitudinal parton distributions, Eq. (24), as a function of the invariant mass of the produced lepton pair (Q^2) at a center of mass energy corresponding to HERA- \vec{N} ($\sqrt{s} = 39.2$) GeV. Notation as in Fig. 2. Error bars have been calculated at LO and include acceptance corrections. Error bars in the lower curve have been slightly shifted to appreciate the overlap.

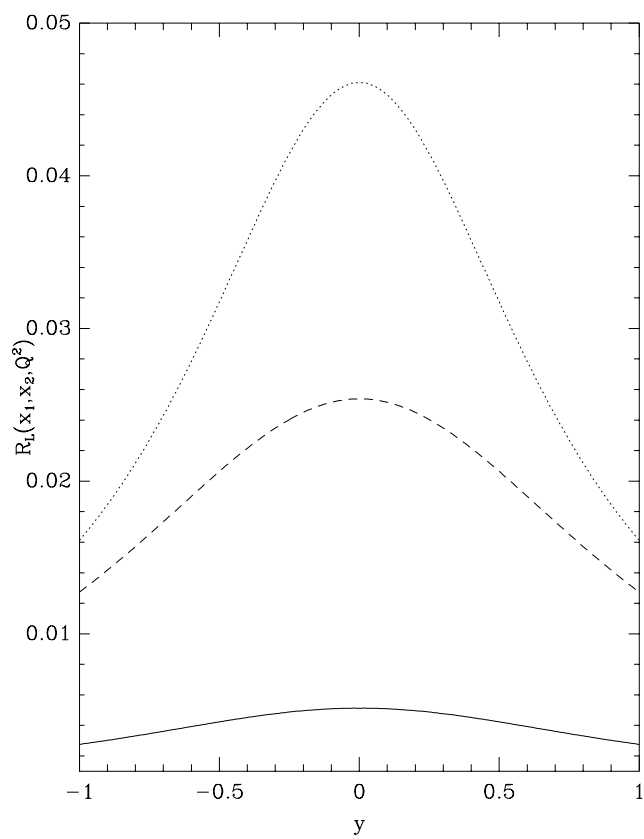


(a)

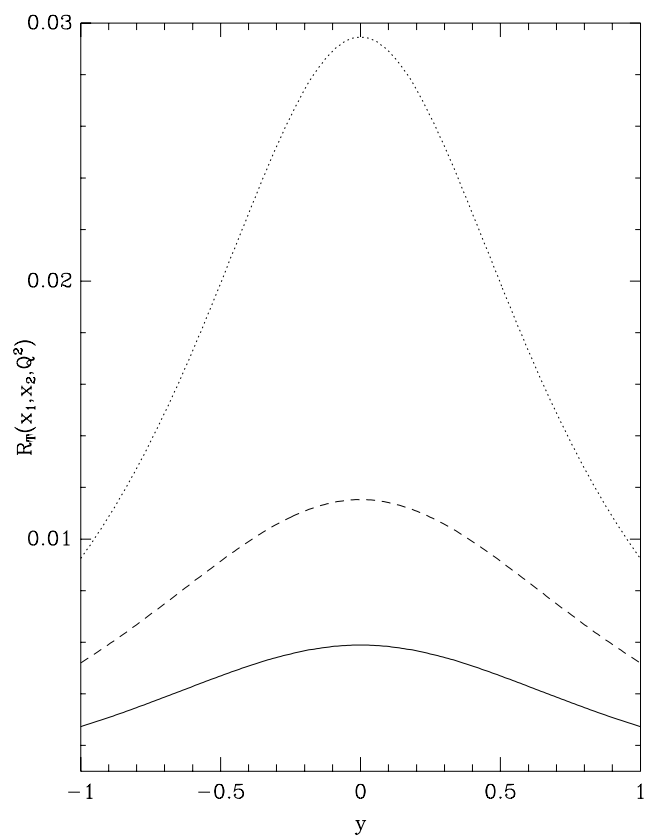


(b)

Figure 1



(a)



(b)

Figure 2

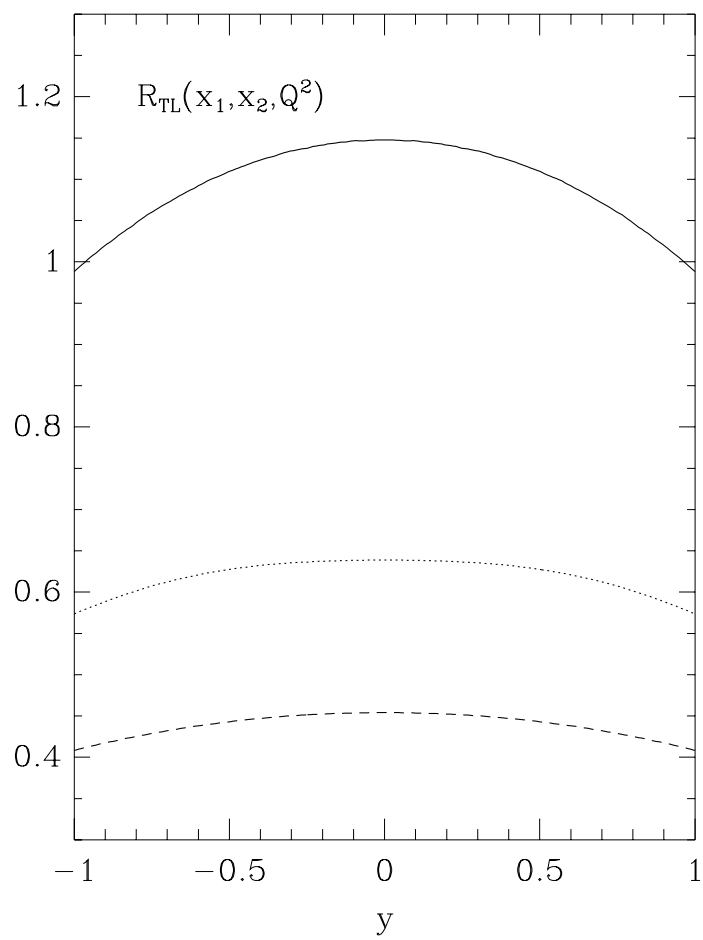


Figure 3

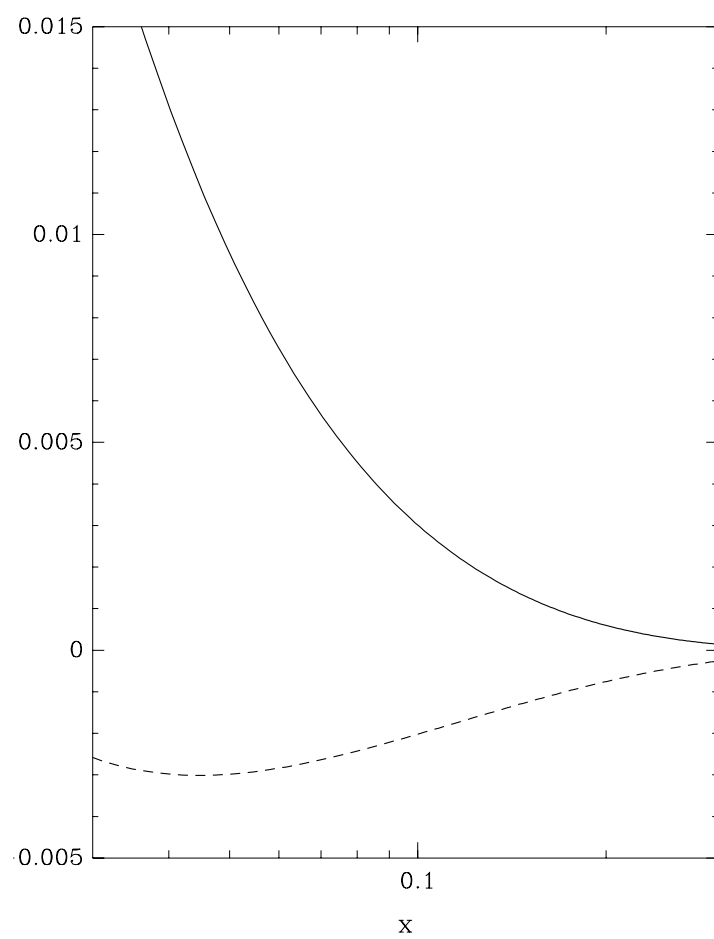


Figure 4

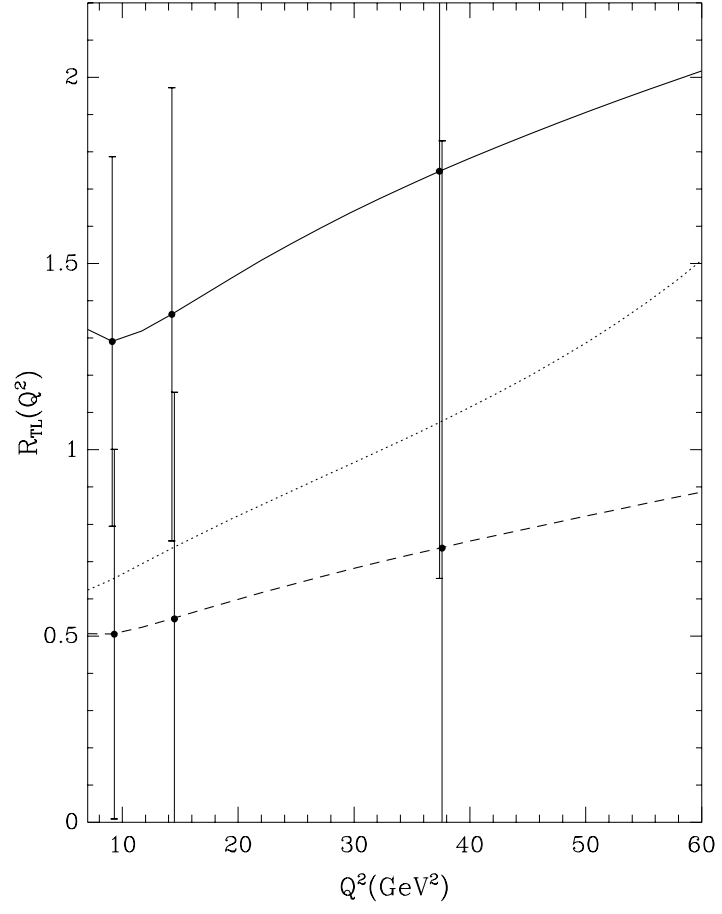


Figure 5